Surface analysis of a heat-treated, Al-containing, iron-based superalloy

M. F. López, A. Gutiérrez, M. C. García-Alonso, and M. L. Escudero
Departamento de Corrosión y Protección, Centro Nacional de Investigaciones Metalúrgicas, C.S.I.C., Avda. Gregorio del Amo 8, 28040 Madrid, Spain

(Received 11 July 1997; accepted 18 January 1998)

The surface composition of MA 956 superalloy both as-received and after four exposure times at 1100 °C has been investigated by energy dispersive x-ray spectrometry (EDX) and x-ray photoelectron spectroscopy (XPS). The passive layer of the as-received sample is mainly formed by Cr- and Fe-oxides. Heat treatment leads to the formation of an alumina layer on which small nodules grow. XPS spectra evidence the presence of titanium and yttrium oxides at the surface of the heat-treated samples, suggesting Y and Ti outward diffusion through the alumina layer. Iron and chromium oxides at the topmost surface layers are observed only for short heat-treatment times.

I. INTRODUCTION

Fe–Cr–Al-based alloys are among the metallic materials with the highest oxidation and corrosion resistance at elevated temperatures. This good resistance arises because alumina scales with excellent thermodynamic stability, and very slow growth rates form during high-temperature exposure. The adherence of these oxide scales to the alloy substrate can be significantly enhanced by adding small amounts of reactive elements, for example yttrium.[1] The incorporation of a small amount (≈0.5 wt. %) of dispersed yttrium oxide[2] also improves the adherence of the oxide layer and gives rise to the development of oxide dispersion strengthened (ODS) alloys. Besides, this dispersed yttrium oxide addition leads to a higher mechanical strength compared with alloys containing metallic yttrium.[3]

Fe–Cr–Al-based ODS alloys are thus widely used for high-temperature applications due to the combination of high-temperature mechanical properties and superior oxidation resistance.[4,5] Additionally, these alloys could also be suitable for room temperature applications due to the formation of the alumina surface layer after high-temperature exposure. For instance, metallic prostheses with ceramic coatings are widely used nowadays due to their excellent biological compatibility and corrosion resistance in physiological media.[6,7] The iron-based MA 956 superalloy develops an adherent alumina layer at the surface after heat treatment at 1100 °C. The use of this commercial superalloy as surgical implant has been recently proposed due to its excellent corrosion resistance in physiological solutions.[8,9] In order to consider this preoxidized superalloy as possible biomaterial, a mechanical study of this superalloy is also being performed.[10] A detailed determination of the near-surface composition is also essential for a complete characterization of this possible biomaterial because the most external layers will be in direct contact with the biological tissues in the *in vivo* experiments.

The aim of this work is to study the composition of the outermost layers of the MA 956 superalloy after four different exposure times at 1100 °C and, for comparison, in the as-received condition.

II. EXPERIMENTAL

The MA 956 superalloy, with chemical composition Fe–20Cr–5Al–0.5Ti–0.5Y_2O_3 (wt. %), was supplied by Inco Alloys International (Hereford, U.K.). Samples were abraded, polished until reaching an average roughness value of $R_a = 0.2$ μm, and ultrasonically cleaned in ethanol before exposition at high temperature. The material in this state was labeled as the *as-received* sample. At this time, different samples were annealed at 1100 °C in air for four different exposure times, 3, 10, 50, and 100 h. After heat treatment, samples were removed from the furnace and air cooled.

The composition and morphology of the surface were analyzed by using scanning electron microscopy (SEM) and energy dispersive x-ray spectrometry (EDX) on the samples after the surface was gold coated to make it conducting. X-ray photoelectron spectroscopy (XPS) was used to analyze the composition of the topmost surface layers.

XPS spectra were recorded under ultra-high vacuum (UHV) conditions using a Mg x-ray source and a VG-CLAM hemispherical electron energy analyzer equipped with a special lens to probe small areas on the sample (<1 mm^2). The base pressure in the UHV chamber during measurements was better than 1×10^{-9} mbar. Samples were cleaned by Ar^+-sputtering for 2 min with an ion gun operating at a sample current of 1 μA, an ion energy of 3 keV, and a sputter rate of approximately

1.5 Å min^{-1}. The total spectral resolution of the XPS measurement was ≈0.6 eV.

III. RESULTS AND DISCUSSION

The high-temperature oxidation of this Fe–Cr–Al base alloy mainly involves the formation of an alumina scale on the material surface. The thickness of the oxide layer after heat treatment at 1100 °C for 3 h is ≈1 μm, and for 100 h ≈5 μm, as has been observed in transversal sections by SEM.[11] Figures 1(a) and 1(b) show two SEM images of the surface obtained for samples treated at 1100 °C for 3 and 100 h, respectively. The alloy surface consists in both cases of a flat alumina base scale on which small nodules have grown. For both exposure times, nodules with different sizes can be observed. The size of these nodules, however, increases with the exposure time, as can be seen comparing Figs. 1(a) and 1(b). The presence of the oxide nodules could benefit the osseointegration process of this possible biomaterial due to the roughness conferred to the surface. On the other hand, the composition of these nodules is very important in biomedical applications because they might lead to toxicity problems by ion release.

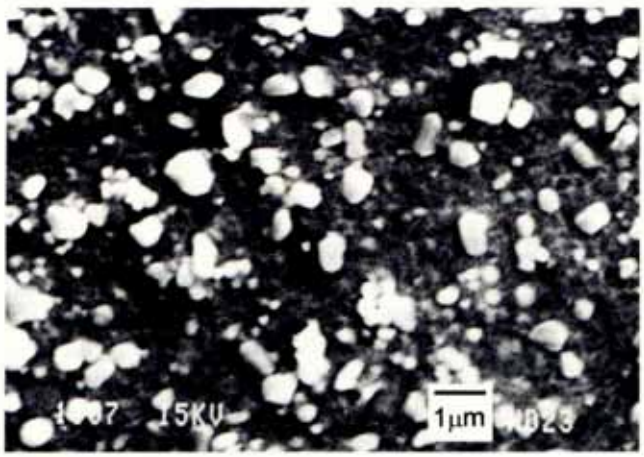

(a)

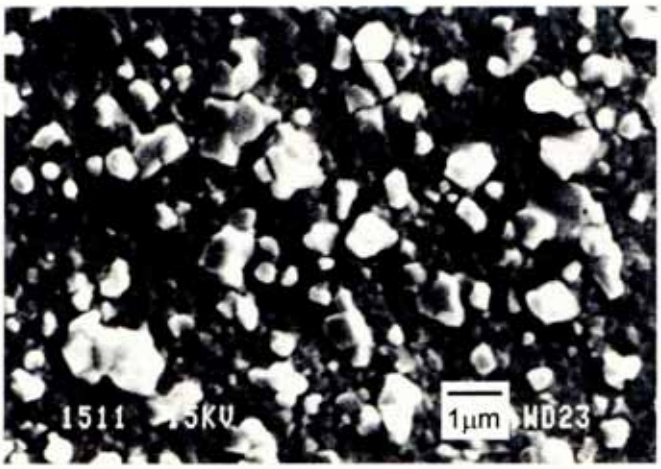

(b)

FIG. 1. SEM micrograph of the surface of the ODS MA 956 heat treated at 1100 °C for (a) 3 h and (b) 100 h.

Figures 2(a) and 2(b) show EDX spectra of large and small nodules, respectively, for samples treated at 1100 °C for 3 h. The signal corresponding to Au is due to the gold deposited on the surface to make it conducting. At this short oxidation time, the largest nodules are composed of oxides rich in Fe and Cr, as is shown in Fig. 2(a). However, the smallest nodules are mainly composed of oxides rich in Ti and in minor proportion in Y, as can be observed in Fig. 2(b). The composition of the nodules observed by EDX on samples treated at 1100 °C for 100 h is represented in Fig. 2(c). As it was shown in Fig. 1(b), for an exposure time of 100 h the surface presents large and small nodules. For this exposure time, and in contrast to the 3 h heat-treated sample, the composition of both large and small nodules is very similar. Figure 2(c) shows that these nodules are mainly composed of Ti and Y with a small amount of Fe and Cr. The spectra shown in Fig. 2 reveal that the composition of the nodules depends on the oxidation time. In order to clarify the evolution of the composition of the topmost surface layers of the alumina scale for the different oxidation times, XPS has been used.

Figure 3 represents Al-2p XPS spectra of all four heat-treated samples, as well as the as-received sample. The spectrum obtained for the as-received sample is magnified by a factor two in order to distinguish the Al-2p emission clearly. This low Al intensity for the as-received sample indicates that the Al incorporation to the passive layer formed spontaneously on the superalloy surface via air contact is negligible. This magnified spectrum shows two components. The emission at a binding energy (BE) of ≈72.3 eV is related to the metallic or elemental Al-2p contribution, whereas the emission at ≈74.4 eV BE is related to the oxidized contribution. The presence of elemental Al in the passive layer is not expected and, consequently, we assign the elemental component to emission from the alloy base material and not from the passive layer. The rest of the spectra shown in Fig. 3, corresponding to the heat-treated samples, exhibit a large oxidized component, located at 75.2 eV BE, without metallic Al-2p emission. This spectral line shape is similar for all heat-treated samples investigated. This result indicates that, even for the shortest treatment time, i.e., 3 h, the aluminum located near the sample surface is completely oxidized. This conclusion could have been expected taking into account the thickness of the oxide layer, about 1 μm. The energy shift observed between the oxidized component of the as-received and the heat-treated samples is probably related to the presence of low order oxides in the first case.[12]

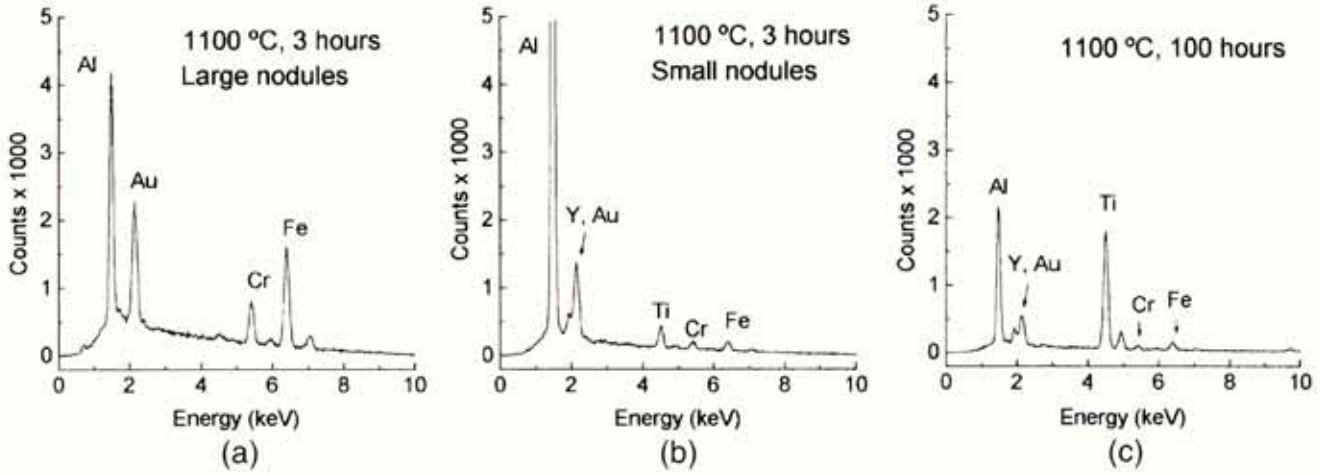

FIG. 2. EDX analysis of the surface of the ODS MA 956 heat-treated at 1100 °C for (a) 3 h (large nodules), (b) 3 h (small nodules), and (c) 100 h.

Figure 4 shows the Cr-2p XPS spectra of all samples. The MA 956 as-received sample exhibits the $2p_{3/2}$ emission at ≈573–579 eV BE and the $2p_{1/2}$ emission at ≈582–588 eV BE. Both emissions, $2p_{1/2}$ and $2p_{3/2}$, have different intensities but their shape is similar and, consequently, the information about the chemical state of chromium at the surface, too. Therefore, we will concentrate on the highest intensity emission, i.e., the $2p_{3/2}$ signal. This emission shows two contributions: a metallic component at ≈574 eV BE, and an oxidized component at ≈576.3 eV BE. The oxidized chromium emission comes from the passive layer formed spontaneously via air contact on the surface of the as-received sample. The metallic Cr component comes from the alloy

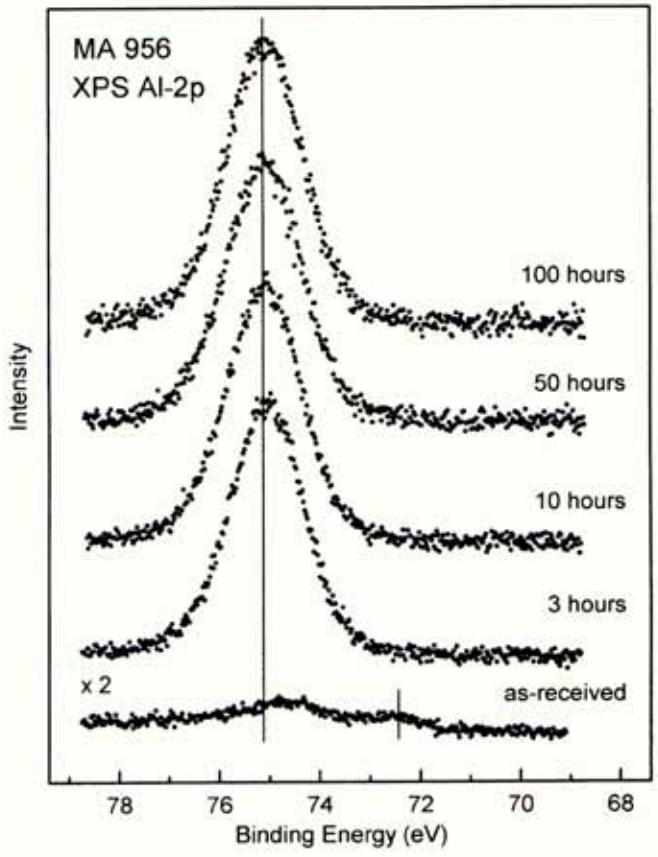

FIG. 3. Al-2p photoelectron spectra of the as-received MA 956 sample and of the heat-treated alloy after four different exposure times: 3, 10, 50, and 100 h.

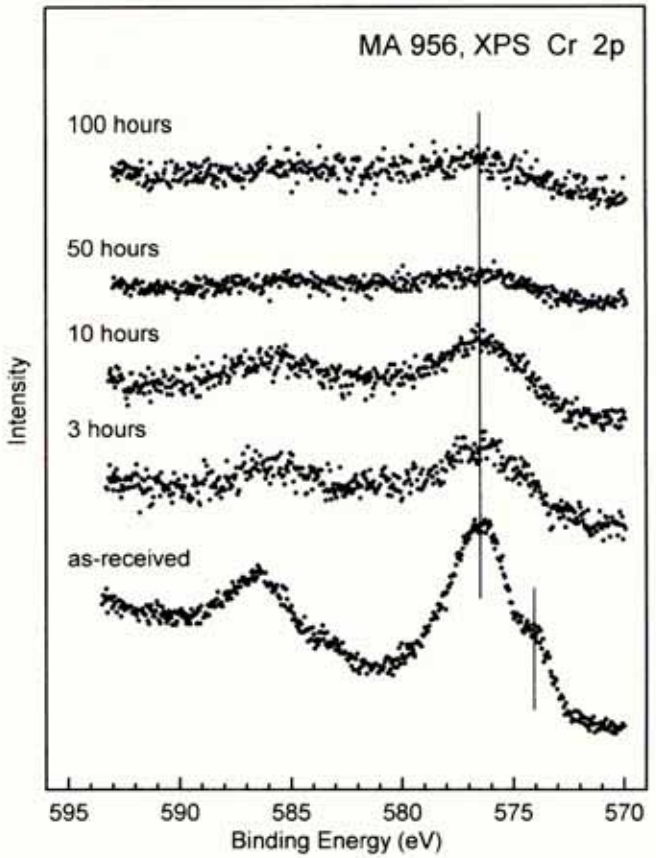

FIG. 4. Cr-2p photoelectron spectra of the as-received MA 956 sample and of the heat-treated alloy after four different exposure times: 3, 10, 50, and 100 h.

base material and not from the passive layer. The spectra of Fig. 4 show that the heat treatment of the MA 956 superalloy reduces the chromium content at the surface of the material. The spectra corresponding to the oxidized samples do not exhibit metallic Cr-2p emission because the outer oxide layer is too thick to allow electrons coming from the base material to escape. The Cr-2p emission decreases by increasing the heat-treatment time and, for 50 h of thermal exposure, this signal becomes negligible. This indicates that no significant Cr-diffusion to the surface occurs in the formation of the oxide layer. The result obtained for short heat-treatment times agrees with our EDX data [Fig. 2(a)] and with the literature, where the signal corresponding to Cr is also observed.[13]

The probe depth of the EDX technique (up to 1 μm) is much larger than that of XPS. Therefore, the XPS results show the absence of chromium oxides at the topmost surface layers for high exposure times, whereas the EDX data [Fig. 2(c)] show a small amount of chromium corresponding to deeper layers. In other studies[13,14] performed with Rutherford Backscattering Spectroscopy (RBS), which is also a very surface sensitive technique, the Cr signal overlaps with the Ti and Fe emissions and, therefore, it is not easily distinguishable from them. Photoelectron spectroscopy is a more suitable technique to determine if there is an enrichment of Cr at the surface because the three emissions corresponding to Cr, Ti, and Fe are well separated. Therefore, our XPS data demonstrate that, for high exposure times (50 and 100 h), the outermost surface layers of the samples do not contain chromium. Some Al-containing alloys develop a passive layer which consists mainly of alumina.[12] When some amount of Cr (≈5 wt. %) is added to these materials, the Cr atoms seem to favor the alumina layer formation at room- and high temperature in such a way that the resulting alumina layer is more protective, but no appreciable incorporation of Cr to the alumina layer occurs.[12,15]

Figure 5 shows the Fe-2p XPS spectra for all samples. As in the Cr-2p case, the analysis will be focused on the $2p_{3/2}$ emission, located at 705–712 eV BE. All Fe-2p photoelectron spectra behave in a similar way to the Cr-2p case. The as-received sample spectrum shows again an oxidized component (≈710 eV) corresponding to the passive layer and a metallic contribution (≈707 eV) coming from the base material. By heating the samples, the metallic component becomes negligible and the Fe-2p emission decreases, ruling out Fe outward diffusion through the alumina layer. These results confirm the formation of Fe and Cr oxide nodules on the alumina layer for short treatment times, as was previously observed by EDX [Fig. 2(a)]. The absence of Fe and Cr photoemission signals for the samples heat treated for 50 and 100 h indicates that the most external

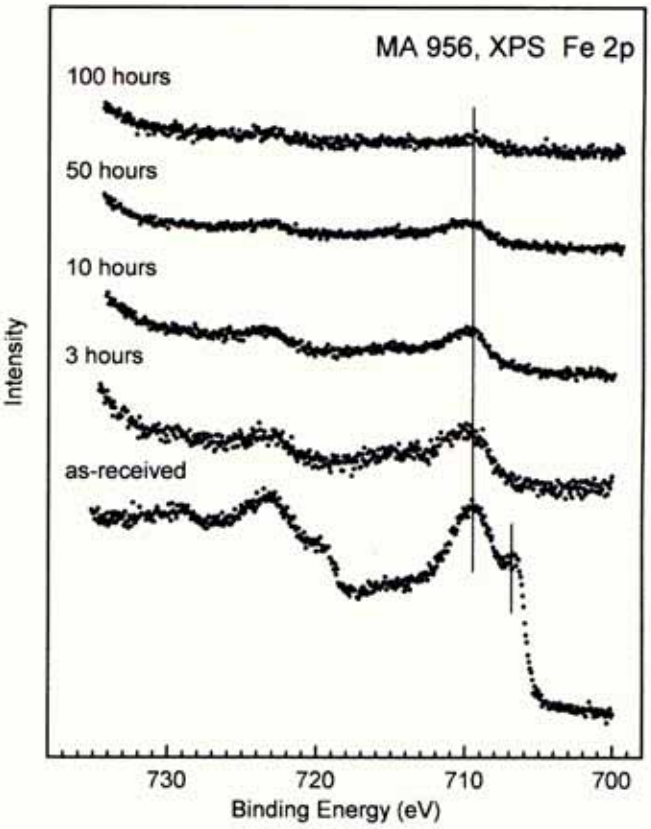

FIG. 5. Fe-2p photoelectron spectra of the as-received MA 956 sample and of the heat-treated alloy after four different exposure times: 3, 10, 50, and 100 h.

layers of these samples do not contain Fe or Cr. However, they can be present in deeper layers, as was observed by EDX [Fig. 2(c)]. This suggests that those Fe and Cr oxide nodules, which are rather voluminous, are not strongly adhered to the alumina layer and, after long heat-treatment exposures, they were detached during the cooling step. These results are in agreement with previous studies performed with RBS, which also showed a decrease of the Fe emission with increasing time.[13,14]

Figures 6 and 7 represent the Ti-2p and Y-3d XPS spectra, respectively, for all samples. In the case of the as-received sample, neither Ti-2p nor Y-3d emissions were detected. This result is expected because of the low Ti and Y_2O_3 content of the superalloy (0.5 wt. %). Besides, this indicates that these elements are not present in the passive layer formed on the material surface. On the other hand, both Ti-2p and Y-3d emissions were detected in the heat-treated samples. Ti-$2p_{3/2}$ (≈458.5 eV BE) and Ti-$2p_{1/2}$ (≈464 eV BE) emissions correspond to oxidized titanium, and no emission from elemental titanium could be observed. This indicates that the chemical state of titanium in the oxide layer of the heat-treated samples corresponds to oxidized Ti, with no contribution from metallic Ti. The highest Ti-2p intensity was found for the case of the 10-h sample. For

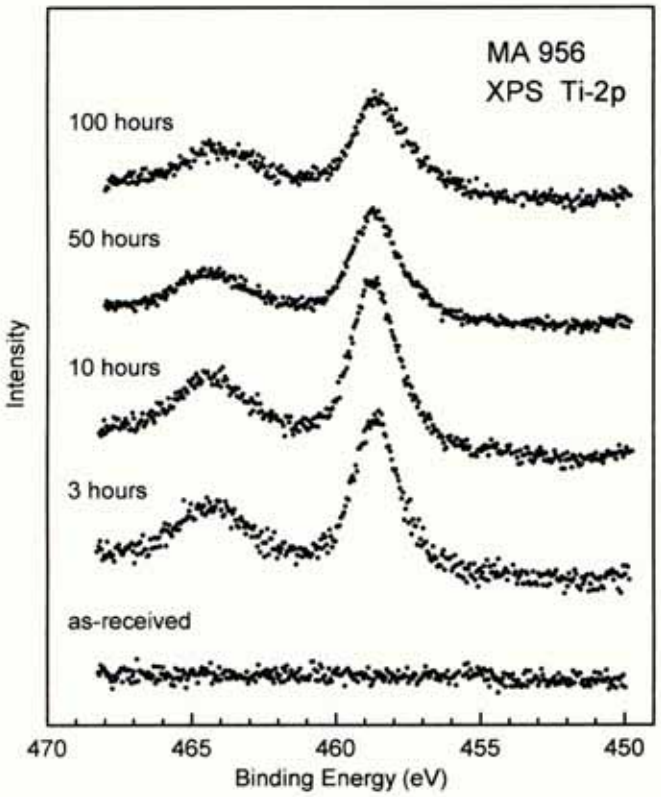

FIG. 6. Ti-2p photoelectron spectra of the as-received MA 956 sample and of the heat-treated alloy after four different exposure times: 3, 10, 50, and 100 h.

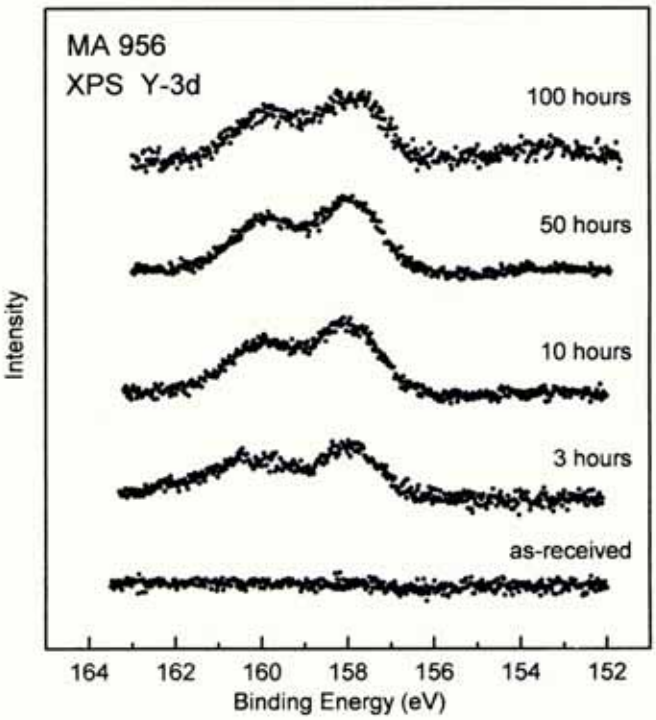

FIG. 7. Y-3d photoelectron spectra of the as-received MA 956 sample and of the heat-treated alloy after four different exposure times: 3, 10, 50, and 100 h.

exposure times longer than 10 h, the Ti-2p emission intensity slightly decreases with the lowest value observed for the 100-h sample. The Y-3$d_{5/2}$ (≈158 eV BE) and the Y-3$d_{3/2}$ (≈160 eV BE) emissions of the heat-treated samples (see Fig. 7) correspond to oxidized yttrium. This emission increases when increasing exposure time up to 10 h treatment time and for higher exposure times remains constant.

As can be seen from Figs. 6 and 7, and according to the results obtained by EDX (Fig. 2) and to previous studies on the MA 956 superalloy after heat treatment at 1100 °C for 3 and 10 h,[4] the presence of small nodules containing titanium and yttrium oxides is confirmed by XPS. Since the probe depth of XPS is much smaller than that of EDX, the XPS results indicate the presence of titanium and yttrium oxides at the topmost surface layers. The presence and subsequent variation of the Y and Ti emission intensities at the surface can be related to the mechanism of formation of the alumina scale. The alumina scale grows by inward oxygen diffusion through grain boundaries toward the scale/metal interface, where new alumina is formed.[4,14] For short treatment times, the alumina scale grain size is small and has equiaxial morphology, but with increasing treatment time the grain size changes along the scale, giving rise to larger and columnar grains at the scale/metal interface.[4]

The presence of Ti and Y on the surface for all treatment times indicates that there is not only oxygen diffusion through the grain boundaries, but also a small but continuous outward diffusion of Y and Ti along the grain boundaries. The fact that the maximum is observed at 10 h, and at longer times the intensity remains constant (in the case of Y) or even slightly decreases (in the case of Ti), can be related to the grain size gradient observed in the scale. When the grain size is small, the outward diffusion of these elements is favored and its concentration at the surface increases as the treatment time increases. However, after 10 h the alumina scale growth leads to larger grains at the scale/metal interface, hindering the diffusion of these elements and, therefore, decreasing their concentration at the surface.

The transport of yttrium from the alloy through the oxide layer is apparently surprising, since yttrium is initially present in the form of very stable dispersed oxide. However, this result is in perfect agreement with previous findings on the diffusion of yttrium through the oxide layer via grain boundaries.[14,16] RBS studies[13,14] have also established that the surface region after heat treatment becomes enriched in yttrium and titanium oxides. These RBS results are in nice agreement with our XPS study.

From the surface analysis performed on the MA956 superalloy thermally treated at 1100 °C for different times, it can be deduced that, between 50 and 100 h

treatment time, the surface presents nodules on the alumina scale formed only by stable Y and Ti oxides. For these exposure times there is no presence of Fe or Cr oxides at the topmost surface layers of the samples. These exposure times provide also an alumina layer with satisfactory thickness and adherence for biomedical applications as surgical implants.[8,11]

IV. CONCLUSIONS

By using XPS it has been shown that the passive layer spontaneously formed on the ODS MA 956 superalloy via air contact is constituted by chromium and iron oxides with a very small amount of Al. Yttrium and titanium emissions could not be detected, indicating no significant incorporation of Y and Ti into the passive layer. The oxidation of the ODS MA 956 superalloy at 1100 °C for four different exposure times gives rise to the formation of an alumina layer on which small nodules are observed. At short treatment times, two different kinds of nodules are observed, which are composed of titanium and yttrium oxides and of iron and chromium oxides, respectively. However, after longer annealing times, all nodules are mainly composed of titanium and yttrium oxides with a small amount of iron and chromium oxides at intermediate depths, as has been observed by EDX.

There seems to be a continuous titanium and yttrium diffusion through the grain boundaries of the alumina scale, which is maximum at 10 h, as has been observed by XPS. For longer annealing times, the diffusion is less favored. The presence of these nodules produces a surface roughness, which is important in biomedical applications because it can favor the osseointegration process. For 50 and 100 h treatment times, the surface is composed of Y and Ti oxides on the alumina scale, with no presence of Fe or Cr oxides at the outermost layers, as evidenced by XPS. Taking into account that titanium and yttrium oxides are rather stable and adherent, in contrast to iron and chromium oxides, the optimal oxidation period to use this oxidized alloy as biomaterial is in the range between 50 and 100 h.

ACKNOWLEDGMENTS

The authors thank J. L. González-Carrasco for his help during EDX and SEM measurements. This work was supported by the project MAT95-0249-C03-01 of the Spanish Comisión Interministerial de Ciencia y Tecnologia (CICYT).

REFERENCES

1. A. M. Huntz, in *Role of Active Elements in the Oxidation Behavior of High Temperature Metals and Alloys*, edited by E. Lang (Elsevier Applied Science, London, 1989), p. 81.
2. M. J. Bennett and M. R. Houlton, in *High Temperature Materials for Power Engineering*, edited by F. Bachelet (Kluwer Academic Publishers, Dordrecht, 1990), p. 189.
3. J. S. Benjamin, in *New Materials by Mechanical Alloying Techniques*, edited by E. Arzt and L. Schulz (DGM, Oberursel, 1990), p. 1.
4. W. J. Quadakkers, Werkst. Korros. **41**, 659 (1990).
5. G. Korb and A. Schwaiger, High Temp.-High Press. **21**, 475 (1989).
6. A. Moroni, V. L. Caja, C. Sabato, E. L. Egger, F. Gottsauner-Wolf, and E. Y. S. Chao, J. Mater. Sci-Mater. M. **5**, 411 (1994).
7. P. Leali Tranquilli, A. Merolli, O. Palmacci, C. Gabbi, A. Cacchioli, and G. Gonizzi, J. Mater. Sci-Mater. M. **5**, 345 (1994).
8. M. L. Escudero, J. L. González-Carrasco, C. García-Alonso, and E. Ramírez, Biomater. **16**, 735 (1995).
9. M. L. Escudero, M. F. López, J. Ruiz, M. C. García-Alonso, and H. Canahua, J. Biomed. Mater. Res. **31**, 313 (1996).
10. J. Chao, J. L. González-Carrasco, J. Ibáñez, M. L. Escudero, and G. González-Doncel, Metall. Mater. Trans. A **27**, 3809 (1996).
11. M. L. Escudero and J. L. González-Carrasco, Biomater. **15**, 1175 (1994).
12. M. F. López, A. Gutiérrez, M. C. García-Alonso, and M. L. Escudero, Solid State Commun. **101**, 575 (1997).
13. W. J. Quadakkers, K. Schmidt, H. Grübmeier, and E. Wallura, Mater. High Temp. **10**, 23 (1992).
14. R. A. Versaci, D. Clemens, W. J. Quadakkers, and R. Hussey, Solid State Ionics **59**, 235 (1993).
15. V. Guttmann, A. Mediavilla, and O. Ruano, Mater. High Temp. **11**, 42 (1993).
16. K. Przybylski, A. J. Garratt-Reed, B. A. Pint, E. P. Katz, and G. J. Yurek, J. Electrochem. Soc. **134**, 3207 (1987).